ЯДЕРНА ФІЗИКА
NUCLEAR PHYSICS

УДК 539.142+539.17 https://doi.org/10.15407/jnpae2025.03.210

Diwanshu[1,*], A. Kumar[1], B. Rohila[1,2], C. Sharma[1], Subodh[1], P. S. Rawat[3], A. Pandey[3], K. Katre[4], H. Arora[5], U. S. Ghosh[4], Yashraj[4], I. Sharma[6], H. P. Sharma[6], S. K. Chamoli[3], S. Kumar[3], R. P. Singh[4], S. Muralithar[4]

[1] *Department of Physics, Panjab University, Chandigarh, India*
[2] *Department of Physics, Maitreyi College, University of Delhi, New Delhi, India*
[3] *Department of Physics and Astrophysics, University of Delhi, New Delhi, India*
[4] *Inter University Accelerator Centre, New Delhi, India*
[5] *Central Michigan University, Michigan, USA*
[6] *Department of Physics, Banaras Hindu University, Varanasi, India*

*Corresponding author: diwanshusharma96@gmail.com

MEASUREMENT OF EXCITATION FUNCTION IN THE $^{16}O + ^{107}Ag$ SYSTEM AT ENERGIES ABOVE THE COULOMB BARRIER

The decay mechanism of the highly excited compound nucleus ^{123}Cs populated via fusion evaporation reaction of ^{16}O and ^{107}Ag is studied. De-excitation of the compound nucleus via evaporation of p, n, and α-particles leads to a population of several neutron-deficient residual nuclei. The excitation function for the $^{16}O + ^{107}Ag$ reaction has been determined experimentally in the energy range 71 - 80 MeV above the Coulomb barrier. The experimental results have been analyzed within the framework of statistical codes PACE4 and CASCADE.

Keywords: excitation function, compound nucleus, PACE4, CASCADE.

1. Introduction

Heavy ion induced reactions leading to complete fusion (CF) and incomplete fusion (ICF) at energies near and above the Coulomb barrier have been a topic of interest for many years [1 - 4]. The reaction mechanism is dependent on the angular momentum carried by the projectile. In CF, the projectile completely fuses into the target, and the whole angular momentum of the projectile is imparted to the compound nucleus (CN) which must be less than or equal to l_{crit}, on the other hand in the ICF mechanism only a part of projectile is captured by the target nuclei leading to partial transfer of momentum and the angular momentum lies between l_{crit} and l_{max} [5]. Among the two mechanisms, CF reactions have a higher probability of populating neutron-deficient residual nuclei over the ICF reactions. The CN with high excitation energy and large angular momentum populated in the CF reaction de-excites by evaporating light nuclear particles and discrete γ-rays, resulting in residual nuclei [6 - 9]. Detection of discrete γ-rays following these nuclei forms the basis of gamma-spectroscopy. In γ-ray spectroscopy, it is important to populate the nuclei of our interest with the maximum cross-section. Therefore, measurements of the cross-sections of different decay channels of CN play an important role in planning the γ-spectroscopy experiment for nuclear structure study. Different statistical codes like Projection Angular-momentum Coupled Evaporation (PACE4) [10] and CASCADE [11] are available for the theoretical estimation of the cross-section of populated channels. Therefore, it is important to compare the theoretically predicted cross-sections with the measured cross-sections in order to plan the γ-ray spectroscopy experiment to study the nuclear structure of the nucleus of interest.

In the present article, a detailed analysis of the de-excitation of CN ^{123}Cs through different channels has been done by studying the γ-decay of residual nuclei. The theoretical results predicted by statistical codes were compared with the experimentally measured cross-sections.

2. Experimental details

The present experiment was carried out by using the ^{16}O beam provided by the 15UD Pelletron setup at Inter University Accelerator Centre (IUAC), New Delhi. The beam was impinged on a ~ 1.08 mg/cm^2 thick ^{107}Ag target with a ~ 6.02 mg/cm^2 thick gold backing, leading to the population of ^{123}Cs CN. The beam current was kept to be 2 pnA. The excitation function was performed in the incident beam energy range of 71 - 80 MeV. Beam energies were kept above the Coulomb barrier (~ 49 MeV in laboratory frame) and consequently, the compound nuclei ^{123}Cs were formed with excitation energy in the range 49 - 57 MeV and angular momentum from 31 - 38 ħ.

Four dominant evaporation channels: ^{120}Xe (p2n), ^{120}Cs (3n), ^{119}Xe (p3n), and ^{119}I (α) were populated in the decay of the CN. The γ-rays emitted from the excited states of these residual nuclei were detected by 11 HPGe Clover detectors arranged in INGA [12] set up at IUAC, New Delhi. The data was taken in both single and coincidence mode. The energy and efficiency calibration of clover detectors has been done by using the radioactive ^{152}Eu source of standard γ-energies and intensities. Internal conversion correction has been applied to the intensities of characteristic gamma rays used for the measurement of the cross-sections of different channels. The energy resolution of detectors was ~ 2.5 keV at 1408 keV photopeak of ^{152}Eu. NiasMARS [13] code developed by the IUAC group has been used for data analysis.

3. Theoretical models

Different theoretical codes are available to study the mechanism of fusion-evaporation reaction. In the present work, efforts have been made to study the experimental cross-sections of residues produced in the decay of ^{123}Cs CN populated via $^{16}O + ^{107}Ag$ reaction in the framework of theoretical codes like PACE4 [10] and CASCADE [11].

3.1. PACE4

The statistical fusion-evaporation code PACE4 is a modified version of the JULIAN code and is based on Hauser - Feshbach formalism [14]. It comes preloaded in the LISE ++ utility package and uses Monte-Carlo simulation for the de-excitation of compound nuclei to simulate the main evaporation channels at different beam energies. The transmission coefficients for emitted particles are calculated by the optical model potential [15] while the BASS model [16] is used to measure the CF cross-section. The modified version of the code takes into consideration the excitation energy-dependent level density parameter from S. K. Kataria et al. [17]. The level density parameter is expressed as $a = A/K$, where A is the number of nucleons in the CN and K is a free parameter that can be varied and optimized to reproduce the experimental data. $K = 10$ has been used for the present reaction. It should be noted that ICF and pre-equilibrium emission are not taken into consideration in this code. The ratio of the Fermi gas level density parameter a at the saddle point to the ground state value, known as ARATIO, is taken as unity in the calculations. The classical approach for transmission probability calculations is taken into account for incident energies above the Coulomb barrier. A total of 100000 cascades were used throughout the theoretical calculations done with PACE4.

3.2. CASCADE

CASCADE code is a statistical approach to studying the distributions of the residual nuclei produced via the decay of compound nuclei and measuring the cross-section of long-lived nuclei in the ground state. The decay of a CN is treated in the statistical model using the Hauser - Feshbach [14] formalism, which is applicable for nuclei with high angular momentum. The decay cross-sections are determined by the weight of the final states and the barrier penetrabilities for the various channels. Level densities of residual nuclei are energy-dependent parameters and can be determined under the framework of the Fermi-gas model. At high excitation energies, nuclei are supposed to behave as predicted by the Liquid Drop Model. The transmission coefficients used for the particles evaporating from the CN were calculated by the optical model. For the neutrons' potential given by D. Wilmore and P. E. Hogson [18], for the protons' potential given by C. M. Perey [15], and for the α-particles' potential given by J. R. Huizenga and G. Igo [19], is considered. In the code CASCADE, the level density parameter constant (K) and the ratio of the actual moment of inertia to the rigid body moment of inertia of the excited system (F_θ) are important input parameters and can be varied to reproduce the measured excitation function. In the present work, the level density parameter $a = A/10$ is used for all the CASCADE calculations. It should be noted that ICF and pre-equilibrium emission are not taken into account in this code.

4. Results and discussion

To understand the phenomena involved in the fusion of $^{16}O + ^{107}Ag$ asymmetric system, the determination of the angular momentum of CN plays a significant role. Angular momentum calculation has been carried out by the dynamical model HICOL [20, 21] and has been compared with the angular momentum given by CASCADE for a wide range of energies. The difference between the two is that CASCADE gives the angular momentum of the CN, while HICOL gives a more realistic picture and predicts angular momentum that contributes to the fusion. It can be seen clearly from Fig. 1, *a* that in the lower energy range, HICOL predicts that the higher values of angular momentum contribute to the fusion as compared to classically predicted values. In the higher energy range (> 120 MeV), the l_{max} predicted by HICOL is less than the angular momentum predicted by CASCADE and almost saturates. Also, Fig. 1, *b* shows the evolution of the distance between fusing nuclei with time for different values of l. It can be concluded from the plot that angular momentum up to l_{max} (= 36 ħ) for that particular energy contributes to the CN, leading to fusion. From these results, we can conclude that at higher energy range, ICF is the dominant phenomenon whereas in lower energy range $E \sim 71$ - 80 MeV (region of our interest), the incident projectile is completely fusing into target nuclei and imparts its entire momentum to CN and hence leads to the CF mechanism for our system.

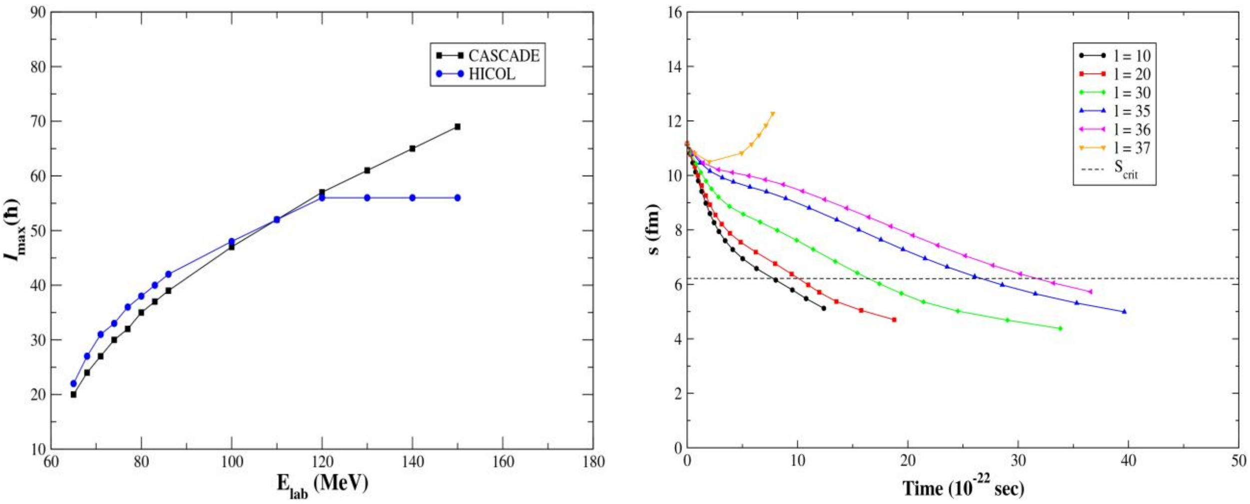

a *b*

Fig. 1. *a* - Variation of angular momentum l_{max} with respect to incident energy E_{lab};
b - evolution of separation (*s*) as a function of time at 77 MeV for asymmetric system $^{16}O + ^{107}Ag$.
(See color Figure on the journal website.)

The CN ^{123}Cs populated in the $^{16}O + ^{107}Ag$ reaction decay by emission of light particles, i.e., protons, neutrons, and α-particles. In the present work, the excitation function of four evaporation residues produced in (^{16}O, p2n), (^{16}O, 3n), (^{16}O, p3n), and (^{16}O, α) reaction channels in the incident energy range 71 - 80 MeV has been measured. The residues were identified by their characteristic γ-rays marked in the spectra obtained as shown in Fig. 2. The nuclear spectroscopic data [22 - 25] used in the present work to calculate the residual cross-sections are listed in Table 1.

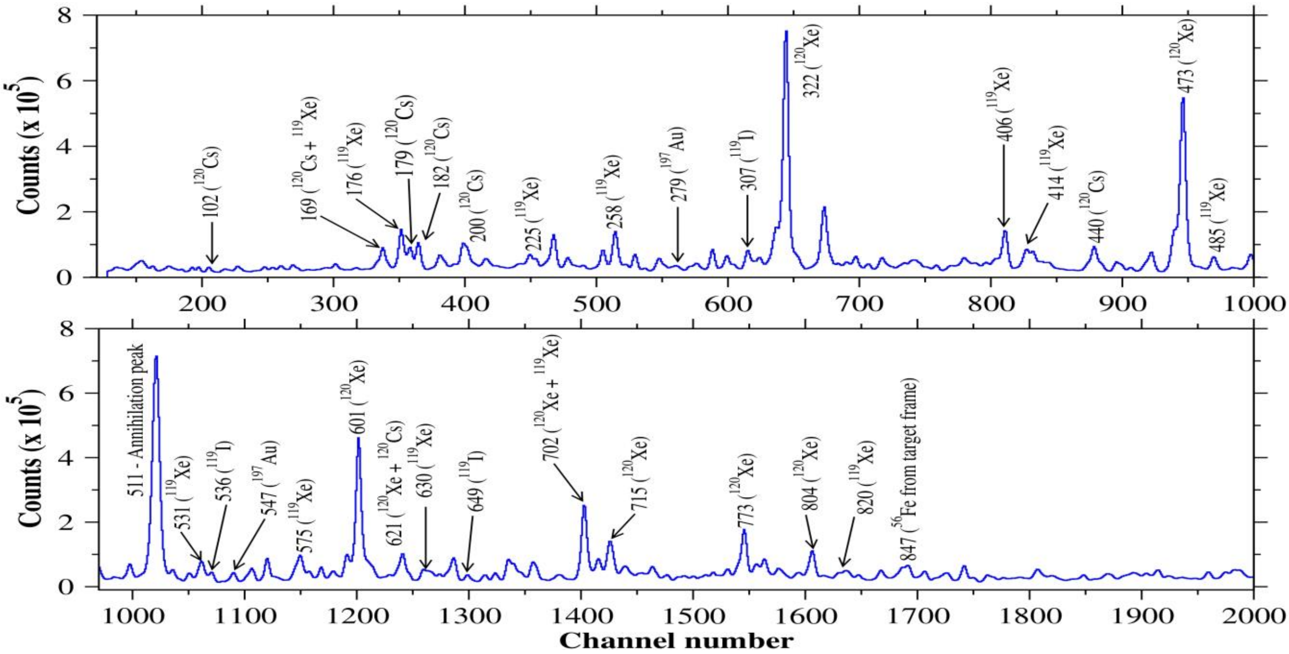

Fig. 2. A typical γ-ray spectrum obtained in the $^{16}O + ^{107}Ag$ reaction at beam (^{16}O) energy = 77 MeV.
The γ-ray peaks of populated nuclei are marked in the spectrum with their energy in kilo-electronvolt.
(See color Figure on the journal website.)

Table 1. **Nuclear spectroscopic data used for the cross-section evaluation in the present paper**

Residue	J^π	E_γ, keV
^{120}Xe	0^+	322.6 876.1
^{120}Cs	7^-	102.4 179.4
^{119}Xe	$5/2^+$	176.08 225.13 485 459 257.9 169
^{119}I	$5/2^+$	99 307 536 650

The relative experimental cross-sections corresponding to various evaporation residues are determined by measuring the intensities of these γ-rays. The yield of each residual nucleus is measured from the background-subtracted peak area count of the particular characteristic γ-ray. The area of peaks has been converted into relative experimental cross-sections after applying internal conversion correction to the intensities and detector efficiency corrections. The cross-sections for all the isotopes obtained in this way have been normalized to 100 % for ^{120}Xe at 74 MeV. The experimentally measured cross-sections with their errors are quoted in Table 2. Normalization has been done separately for PACE4 and CASCADE.

Table 2. **Measured relative residual cross-sections (mb) at different incident energies**

E_{lab}, MeV	σ (^{120}Xe)	σ (^{120}Cs)	σ (^{119}Xe)	σ (^{119}I)
71 ± 1.3	117.6 ±12.9	43.7 ±5.2	40.8 ± 4.9	25.4 ± 3.2
74 ± 1.3	100.0 ±11.5	41.6 ±5.0	73.6 ± 8.5	30.1 ± 3.6
77 ± 1.3	70.9 ± 8.3	27.4 ±3.4	88.2 ± 10.1	35.3 ± 4.1
80 ± 1.3	24.0 ± 3.0	16.7 ± 2.2	110.9 ± 12.5	41.6 ±5.0

The errors and uncertainties in the measurement of fusion cross-sections may depend on different factors:

– systematic error in the measurement of target thickness is calculated to be less than 3 %;

– statistical errors in the determination of gamma yield were minimized by taking data for comparatively longer period;

– error in determination of geometry dependent detector efficiency is estimated to be ≤ 5 %;

– uncertainty may arise due to fluctuations in beam current and were minimized by continuously monitoring it and keeping it constant. Error due to this factor is estimated to be less than 4 %;

– error in incident beam energy is estimated to be less than 2 %.

4.1. p2n channel

Before comparing the measured excitation functions with the theoretical predictions, it is important to check the impact of input parameters used in PACE4 and CASCADE on the residual excitation function to get their optimized value for further calculations. For this purpose, variation of the theoretical cross-section for p2n channel (^{120}Xe) with the beam energy is analyzed at different level density parameters $K = 8$, 9, and 10 used in PACE4 and shown in Fig. 3. Although there is no significant variation among the three K values at higher energies, small deviation is observed at lower energies below 74 MeV. It is clear from the Figure that the theoretical cross-section corresponding to $K = 10$ seems to reproduce the experimentally measured cross-section, and therefore, is accepted as the optimum choice for further calculations. For the CASCADE code, parameter F_θ is found to affect the excitation function, as can be seen in Fig. 4. The comparison between experimental results and CASCADE predictions has been done at $F_\theta = 0.65$, 0.85, and 0.95. Among all the values, $F_\theta = 0.95$ seems to reside closer to the experimental excitation function and is therefore considered the best value for further calculations.

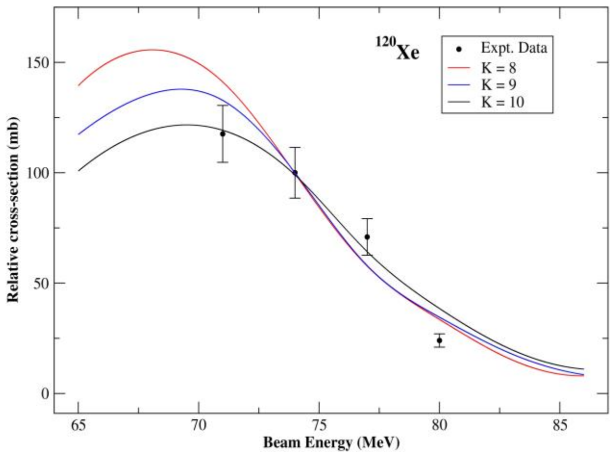

Fig. 3. Comparison of measured relative cross-sections of p2n channel (^{120}Xe) and PACE4 calculations with K = 8, 9, and 10. (See color Figure on the journal website.)

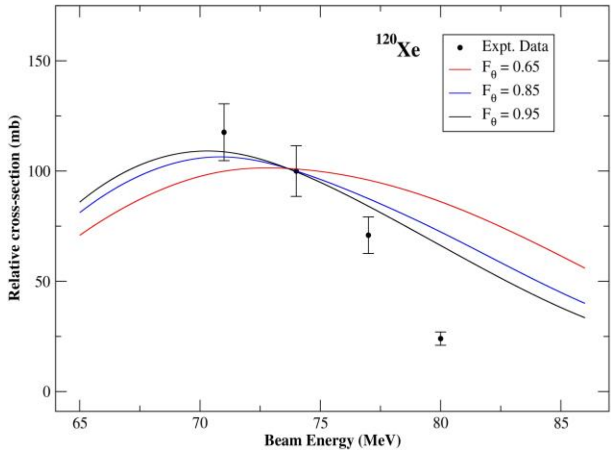

Fig. 4. Comparison of measured relative cross-sections of p2n channel (^{120}Xe) and CASCADE calculations with F_θ = 0.65, 0.85, and 0.95. (See color Figure on the journal website.)

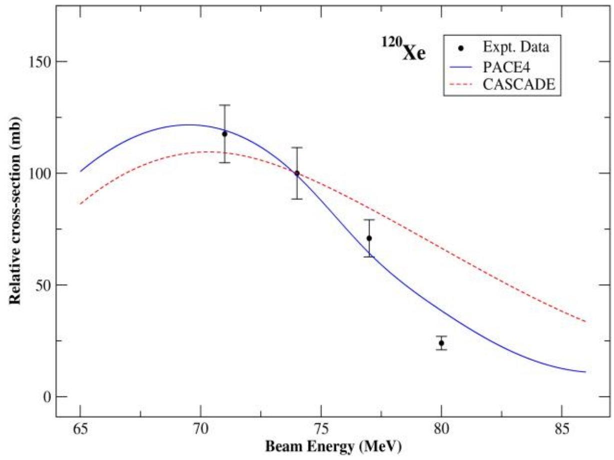

Fig. 5. Comparison of measured relative residual cross-sections (*solid black circle*) for p2n channel with theoretically predicted PACE4 (*solid blue line*) and CASCADE (*dotted red line*) results. (See color Figure on the journal website.)

Fig. 5 shows the comparison of the excitation function for ^{120}Xe produced via ^{107}Ag(^{16}O, p2n) ^{120}Xe, where the black circle denotes the experimental data with an error bar, the solid blue line and dotted red line show the theoretical calculations by PACE4 and CASCADE, respectively. It is clear from Fig. 5 that the theoretically calculated excitation function by PACE4 corresponding to $K = 10$ seems to reproduce the excitation function of residue ^{120}Xe produced via CF of ^{16}O and ^{107}Ag. CASCADE (*dotted red line*) seems to agree with the experimental data at the two lower energies and then starts to deviate from the data at higher energies (> 77 MeV).

4.2. 3n channel

The decay of CN ^{123}Cs populated via CF of ^{16}O in ^{107}Ag, via 3n channel, leads to the formation of ^{120}Cs nuclei whose excitation function has been presented in Fig. 6.

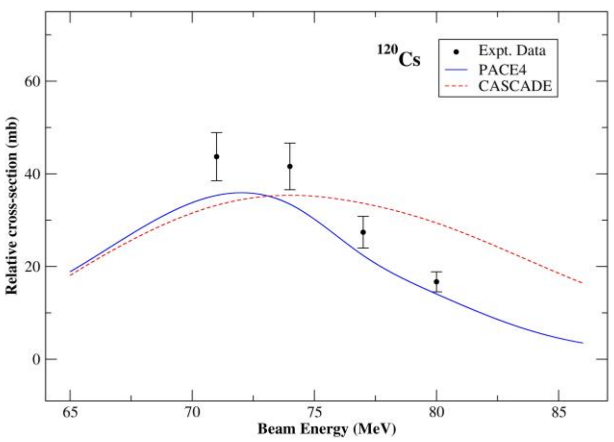

Fig. 6. Comparison of measured relative residual cross-sections (*solid black circle*) for 3n channel with theoretically predicted PACE4 (*solid blue line*) and CASCADE (*dotted red line*) results. (See color Figure on the journal website.)

It has been observed that PACE4 gives a good agreement to the experimental data. On the other hand, CASCADE follows an opposite trend as predicted by experimental and PACE4 calculations. It underpredicts the data at energies below 74 MeV and overpredicts the data at higher energies.

4.3. p3n channel

The measured excitation function of ^{119}Xe produced through ^{107}Ag(^{16}O, p3n)^{119}Xe channel, along with theoretical predictions, is presented in Fig. 7.

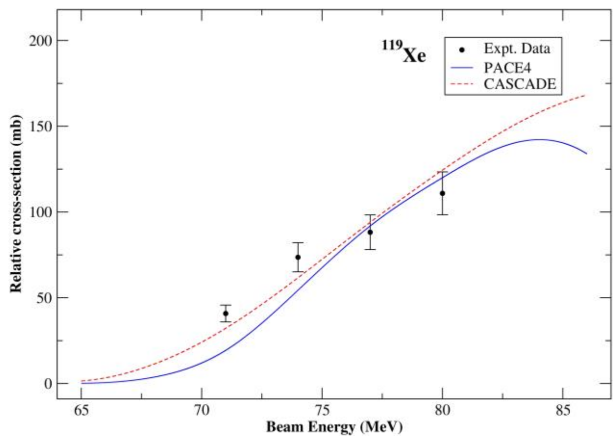

Fig. 7. Comparison of measured relative residual cross-sections (*solid black circle*) for p3n channel with theoretically predicted PACE4 (*solid blue line*) and CASCADE (*dotted red line*) results. (See color Figure on the journal website.)

PACE4 and CASCADE calculations follow the same trend and satisfactorily reproduce the experimentally measured cross-section at all the energies.

4.4. α channel

A comparison of measured excitation function along with theoretical predictions for evaporation residue ^{119}I formed by the decay of CN ^{123}Cs through α channel is represented in Fig. 8. It has been observed that CASCADE calculations satisfactorily reproduce the experimental data except at the lowest energy point (E = 71 MeV) while PACE4 underpredicts the data at two lower energies and overpredicts at the other two higher energies.

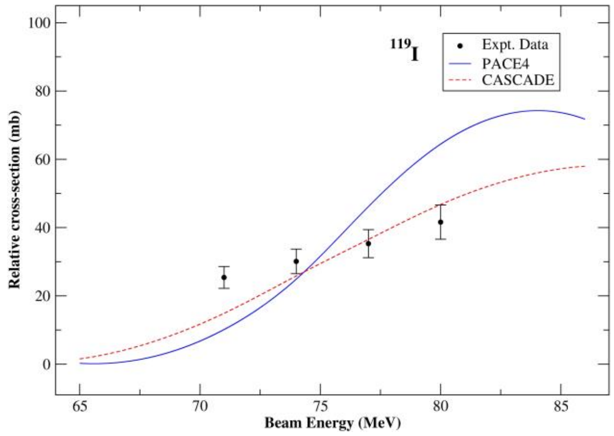

Fig. 8. Comparison of measured relative residual cross-sections (*solid black circle*) for the α channel with theoretically predicted PACE4 (*solid blue line*) and CASCADE (*dotted red line*) results. (See color Figure on the journal website.)

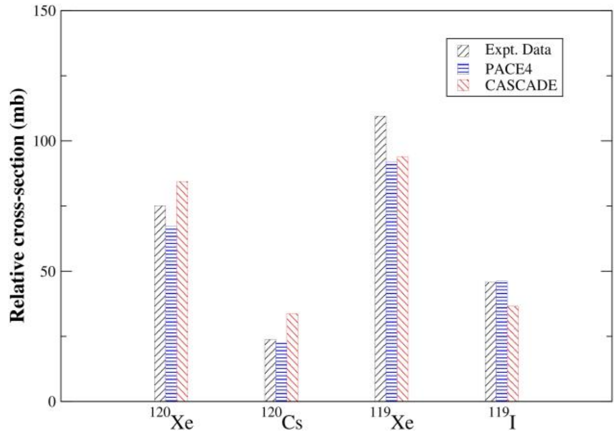

Fig. 9. Comparison of the relative residual cross-sections obtained experimentally and from PACE4 and CASCADE at E beam = 77 MeV. (See color Figure on the journal website.)

Fig. 9 shows the comparison of the relative cross-section for all the residual nuclei populated in the experiment at incident beam energy 77 MeV. It can be concluded from the Figure that the experimentally measured relative cross-section agrees well with the PACE4 results except only for ^{119}Xe. These calculations helped in planning the γ-spectroscopy experiment to populate the nucleus of interest at E_{lab} = 77 MeV.

5. Conclusion

The reaction mechanism of the HI-induced reaction leading to CF is studied in the framework of codes HICOL and CASCADE. The decay of CN ^{123}Cs via different channels is analyzed, and the experimentally measured excitation function of four evaporation residues ^{120}Xe, ^{120}Cs, ^{119}Xe, and ^{119}I, formed in the CF reaction, is studied at several beam energies ranging from 71 - 80 MeV. Theoretical cross-section values as predicted by statistical codes PACE4 and CASCADE were compared with the experimentally obtained results. It was found that PACE4 results are closer to the experimental data in comparison with CASCADE using the default parameters in both codes. Therefore, PACE4 predictions were considered to plan the experiment for populating nuclei of interest with maximum cross-section.

We would like to acknowledge the support from Pelletron staff at IUAC, New Delhi, for providing the stable beam of ^{16}O throughout the experiment, and the INGA collaboration for their help. One of the authors (Diwanshu) acknowledges the financial support received from DST-INSPIRE in the form of a research fellowship (INSPIRE Code IF170914).

REFERENCES

1. P.P. Singh et al. Role of high *l* values in the onset of incomplete fusion. Phys. Rev. C 80 (2009) 064603.
2. P.P. Singh et al. Observation of complete- and incomplete-fusion components in ^{159}Tb,$^{169}Tm(^{16}O, x)$ reactions: Measurement and analysis of forward recoil ranges at E/A ≈ 5 - 6 MeV. Eur. Phys. J. A 34 (2007) 29.
3. D.J. Parker et al. Complete and incomplete fusion in $^{12}C + ^{51}V$ at E(^{12}C) = 36 - 100 MeV from analysis of recoil range and light particle measurements. Phys. Rev. C 30 (1984) 143.
4. D.R. Zolnowski et al. Evidence for “massive transfer” in heavy-ion reactions on rare-earth targets. Phys. Rev. Lett. 41 (1978) 92.
5. E.A. Bakkum et al. Impact parameter dependence of incomplete fusion between 10 and 20 MeV/nucleon. Phys. Rev. C 39 (1989) 2094.
6. B. Fornal et al. Possible dynamic effects in the particle decay of ^{59}Cu compound nuclei. Phys. Rev. C 40 (1989) 664.
7. R.J. Charity. A systematic description of evaporation spectra for light and heavy compound nuclei. Phys. Rev. C 82 (2010) 014610.

8. S. Kundu et al. Deformation in $^{28}Si^*$ produced via the ^{16}O + ^{12}C reaction. Phys. Rev. C 87 (2013) 024602.
9. A. Gavron. et al. Neutron emission in ^{12}C + ^{158}Gd and ^{13}C + ^{157}Gd reactions between 8 and 12 MeV/nucleon. Phys. Rev. C 24 (1981) 2048.
10. A. Gavron. Statistical model calculations in heavy ion reactions. Phys. Rev. C 21 (1980) 230.
11. F. Pühlhofer. On the interpretation of evaporation residue mass distributions in heavy-ion induced fusion reactions. Nucl. Phys. A 280 (1977) 267.
12. S. Muralithar et al. Indian National Gamma Array at Inter University Accelerator Centre, New Delhi. Nucl. Instrum. Methods A 622 (2010) 281.
13. Inter-University Accelerator Centre (IUAC). Data Support Labs.
14. W. Hauser, H. Feshbach. The inelastic scattering of neutrons. Phys. Rev. 87 (1952) 336.
15. C.M. Perey, F.G. Perey. Compilation of phenomenological optical-model parameters 1954-1975. At. Data Nucl. Data Tables 17 (1976) 1.
16. R. Bass. Nucleus-nucleus potential deduced from experimental fusion cross sections. Phys. Rev. Lett. 39 (1977) 265.
17. S.K. Kataria, V.S. Ramamurthy, S.S. Kapoor. Semiempirical nuclear level density formula with shell effects. Phys. Rev. C 18 (1978) 549.
18. D. Wilmore, P.E. Hodgson. The calculation of neutron cross-sections from optical potentials. Nucl. Phys. 55 (1964) 673.
19. J.R. Huizenga, G. Igo. Theoretical reaction cross sections for alpha particles with an optical model. Nucl. Phys. 29 (1962) 462.
20. H. Feldmeier. Transport phenomena in dissipative heavy-ion collisions: the one-body dissipation approach. Rep. Prog. Phys. 50 (1987) 915.
21. N.K. Rai, V. Mishra, A. Kumar. Effect of energy variation on the dissipative evolution of the system in heavy-ion fusion reactions. Phys. Rev. C 98 (2018) 024626.
22. K. Loewenich et al. In-beam spectroscopy of ^{120}Xe. Nucl. Phys. A 460 (1986) 361.
23. C.-B. Moon et al. Level structure of ^{120}Cs. Nucl. Phys. A 696 (2001) 45.
24. H.C. Scraggs et al. High spin study of ^{119}Xe. Nucl. Phys. A 640 (1998) 337.
25. Y. Liang et al. High-spin spectroscopy of $^{119,121}I$: Prolate and oblate shape coexistence. Phys. Rev. C 45 (1992) 1041.

Діваншу[1,*], А. Кумар[1], Б. Рохіла[1,2], С. Шарма[1], Субодх[1], П. С. Рават[3], А. Пандей[3], К. Катрі[4], Х. Арора[5], У. С. Гош[4], Яшрадж[4], І. Шарма[6], Х. П. Шарма[6], С. К. Чамолі[3], С. Кумар[3], Р. П. Сінгх[4], С. Муралітар[4]

[1] *Факультет фізики, Панджабський університет, Чандігарх, Індія*
[2] *Факультет фізики, коледж Майтреї, Делійський університет, Нью-Делі, Індія*
[3] *Факультет фізики та астрофізики, Делійський університет, Нью-Делі, Індія*
[4] *Міжуніверситетський центр прискорювачів, Нью-Делі, Індія*
[5] *Центральний Мічиганський університет, Мічиган, США*
[6] *Факультет фізики, Бенареський індуїстський університет, Варанасі, Індія*

*Відповідальний автор: diwanshusharma96@gmail.com

ВИМІРЮВАННЯ ФУНКЦІЙ ЗБУДЖЕННЯ В СИСТЕМІ ^{16}O + ^{107}Ag ПРИ ЕНЕРГІЯХ ВИЩЕ ЗА КУЛОНІВСЬКИЙ БАР’ЄР

Досліджено механізм розпаду високозбудженого складеного ядра ^{123}Cs, заселеного внаслідок реакції злиття та випаровування ^{16}O та ^{107}Ag. Зняття збудження складеного ядра через випаровування p, n та α-частинок призводить до утворення кількох нейтронно-дефіцитних залишкових ядер. Функцію збудження для реакції ^{16}O + ^{107}Ag було визначено експериментально в діапазоні енергій 71 - 80 МеВ вище за кулонівський бар’єр. Експериментальні результати були проаналізовані в рамках статистичних кодів PACE4 та CASCADE.

Ключові слова: функція збудження, складене ядро, PACE4, CASCADE.

Надійшла / Received 18.02.2025